JHEP

Published for SISSA by Springer

Received: July 16, 2018
Revised: August 15, 2018
Accepted: August 21, 2018
Published: August 24, 2018

Soft gluon resummation for Higgs boson pair production including finite M_t effects

Daniel de Florian[a] **and Javier Mazzitelli**[b]

[a] *International Center for Advanced Studies (ICAS), ECyT-UNSAM, Campus Miguelete, 25 de Mayo y Francia, (1650) Buenos Aires, Argentina*

[b] *Physik-Institut, Universität Zürich, Winterthurerstrasse 190, CH-8057 Zürich, Switzerland*

E-mail: deflo@unsam.edu.ar, jmazzi@physik.uzh.ch

Abstract: We perform the all orders resummation of threshold enhanced contributions for the Higgs boson pair production cross section via gluon fusion, including finite top quark mass (M_t) effects. We present results for the total cross section and Higgs pair invariant mass (M_{hh}) distribution. We obtain results at next-to-leading logarithmic accuracy (NLL) which retain the full M_t dependence, and are matched to the full next-to-leading order (NLO) prediction. Our NLL+NLO results represent the most advanced prediction with full M_t dependence for this process, and produce an increase of about 4% in the total cross section with respect to the NLO result for LHC energies, and for a central scale $\mu_0 = M_{hh}/2$. We also consistently combine the full NLL with the next-to-next-to-leading logarithmically (NNLL) accurate resummation computed in the Born-improved large-M_t limit, and match it to the next-to-next-to-leading order approximation of ref. [1], so called NNLO$_{\rm FTa}$. We find that the resummation effects are very small at NNLL for $\mu_0 = M_{hh}/2$, in particular below 1% at 13 TeV, indicating that the perturbative expansion is under control. In all cases the resummation effects are found to be substantially larger for the central scale $\mu_0 = M_{hh}$, resulting in a more stable cross section with respect to scale variations than the fixed order calculation.

Keywords: NLO Computations, QCD Phenomenology

ArXiv ePrint: 1807.03704

https://doi.org/10.1007/JHEP08(2018)156

JHEP08(2018)156

Contents

1 Introduction

The study of the properties of the Higgs boson discovered by the ATLAS and CMS collaborations is one of the main goals of the present and future runs of the LHC. Among the different measurements that can help to distinguish between the Standard Model (SM) and new physics scenarios, the measurement of the Higgs self coupling is one of particular interest, as in the SM it is determined by the scalar potential, responsible for the electroweak symmetry breaking mechanism.

The production of Higgs boson pairs provides a direct way of measuring the Higgs trilinear coupling, and the high-luminosity upgrade of the LHC is expected to provide constraints on its value by measuring the double Higgs production cross section [2, 3]. In the SM, the main production mechanism is the fusion of gluons via a heavy quark (mainly top quark) loop, and the corresponding cross section has been computed at leading order (LO) in refs. [4–6]. The QCD corrections for this process have been computed first in the heavy top-quark mass (M_t) limit (HTL), both at next-to-leading order [7] (NLO) and next-to-next-to-leading order [8–12] (NNLO), and more recently the NLO corrections with full M_t dependence also became available [13, 14], later also supplemented by transverse momentum resummation [15] and parton shower effects [16, 17]. The size of the QCD corrections was found to be large –about a 70% increase in the total cross section at NLO for LHC energies–, and also the difference with respect to the HTL was found to be significant, the latter being around 15% larger than the full NLO result at 14 TeV.

Very recently, an improved and fully differential NNLO prediction –labeled NNLO$_{\text{FTa}}$ for full-theory approximation, see also refs. [18, 19]– was presented in ref. [1], which in particular features the full loop-induced double-real corrections. This result predicts an additional increase in the total cross section with respect to the full NLO calculation of about 12% at the LHC, and a residual uncertainty due to missing finite-M_t effects estimated to be about 2.5%.

JHEP08(2018)156

Besides the previously described fixed-order calculations, the all-orders resummation of soft gluon emissions has also been performed –again within the HTL– at next-to-next-to-leading logarithmic accuracy (NNLL) in refs. [20, 21]. The resummed contributions, which account for the dominant effect of the missing higher-orders in the perturbative expansion in the threshold limit, are found to further stabilize the cross section leading to smaller theoretical uncertainties.

In this work we perform the resummation of the threshold enhanced contributions including finite M_t effects. In particular, up to next-to-leading logarithmic accuracy (NLL) we retain the full M_t dependence, therefore obtaining NLL+NLO results that represent the most advanced prediction computed in the full theory. Finally, by performing matching to the NNLO_{FTa} cross section, we achieve *the state of the art* results for Higgs pair production by reaching NNLL accuracy within the best available approximation for the M_t effects.

This work is organized as follows: in section 2 we collect all the analytical expressions needed to perform threshold resummation up to NNLL, then in section 3 we present our numerical predictions for the LHC and future colliders, and in section 4 we summarize the results.

2 Threshold resummation

We consider the hadronic production of Higgs boson pairs via gluon fusion. The hadronic cross section for a collider center-of-mass energy s_H, differential in the Higgs pair system invariant mass M_{hh}, can be expressed in the following way

$$M_{hh}^2 \frac{d\sigma}{dM_{hh}^2}(s_H, M_{hh}^2) \equiv \sigma(\tau, M_{hh}^2) = \sum_{a,b} \int_0^1 dx_1\, dx_2\, f_{a/h_1}(x_1, \mu_F^2)\, f_{b/h_2}(x_2, \mu_F^2) \times \int_0^1 dz\, \delta\left(z - \frac{\tau}{x_1 x_2}\right) \hat{\sigma}_0\, z\, G_{ab}(z; \alpha_S(\mu_R^2), M_{hh}^2/\mu_R^2; M_{hh}^2/\mu_F^2)\,, \tag{2.1}$$

where $\tau = M_{hh}^2/s_H$, μ_R and μ_F are the renormalization and factorization scales respectively, and $\hat{\sigma}_0$ represents the Born level partonic cross section. The parton densities of the colliding hadrons are denoted by $f_{a/h}(x, \mu_F^2)$ with the subscripts a, b labeling the type of massless partons ($a, b = g, q_f, \bar{q}_f$, with $N_f = 5$ different flavours of light quarks). The hard coefficient function G_{ab} can be computed in perturbation theory, expanding it in terms of powers of the ($\overline{\text{MS}}$ renormalized) QCD coupling $\alpha_S(\mu_R^2)$ as:

$$G_{ab}(z; \alpha_S, M_{hh}^2/\mu_R^2; M_{hh}^2/\mu_F^2) = \sum_{n=0}^{+\infty} \left(\frac{\alpha_S}{2\pi}\right)^n G_{ab}^{(n)}(z; M_{hh}^2/\mu_R^2; M_{hh}^2/\mu_F^2)\,. \tag{2.2}$$

We introduce now the notation needed to perform the soft gluon resummation in Mellin space [22, 23]. We start by considering the Mellin transform of the hadronic cross section,

$$\sigma_N(M_{hh}^2) \equiv \int_0^1 d\tau\, \tau^{N-1}\, \sigma(\tau, M_{hh}^2)\,, \tag{2.3}$$

JHEP08(2018)156

which takes the following factorized form

$$\sigma_{N-1}(M_{hh}^2) = \hat{\sigma}_0 \sum_{a,b} f_{a/h_1,\,N}(\mu_F^2)\, f_{b/h_2,\,N}(\mu_F^2)\, G_{ab,\,N}(\alpha_{\rm S}, M_{hh}^2/\mu_R^2; M_{hh}^2/\mu_F^2)\,. \tag{2.4}$$

Here we have introduced the N-moments of the hard coefficient function and parton distributions, specifically

$$f_{a/h,\,N}(\mu_F^2) = \int_0^1 dx\; x^{N-1}\; f_{a/h}(x,\mu_F^2)\,, \tag{2.5}$$

$$G_{ab,\,N} = \int_0^1 dz\; z^{N-1}\; G_{ab}(z)\;\;. \tag{2.6}$$

Once all the ingredients in N-space are known, we can obtain the physical cross section via Mellin inversion,

$$\begin{aligned}\sigma(\tau, M_{hh}^2) = \hat{\sigma}_0 \sum_{a,b} \int_{C_{MP}-i\infty}^{C_{MP}+i\infty} \frac{dN}{2\pi i}\, \tau^{-N+1}\, f_{a/h_1,\,N}(\mu_F^2)\, f_{b/h_2,\,N}(\mu_F^2) \\ \times\; G_{ab,\,N}(\alpha_{\rm S}, M_{hh}^2/\mu_R^2; M_{hh}^2/\mu_F^2)\,,\end{aligned} \tag{2.7}$$

where the constant C_{MP} defining the integration contour in the N-plane is on the right of all the possible singularities of the integrand [24].

We will perform the all-order summation of the threshold enhanced contributions, which corresponds to the limit $z \to 1$ or equivalently $N \to \infty$ in Mellin space, and appear as $\alpha_{\rm S}^n \ln^m N$ terms with $1 \le m \le 2n$. We will therefore consider (for the resummed contributions) only the gluon-initiated configuration, given that it is the only partonic channel that is not suppressed in this limit. The soft-gluon contributions in the large-N limit can be organized in the following all-order resummation formula for the partonic coefficient function in Mellin space,

$$\begin{aligned}G_{gg,\,N}^{(\rm res)}(\alpha_{\rm S}, M_{hh}^2/\mu_R^2; M_{hh}^2/\mu_F^2) = C_{gg}(\alpha_{\rm S}, M_{hh}^2/\mu_R^2; M_{hh}^2/\mu_F^2) \\ \cdot\, \Delta_N(\alpha_{\rm S}, M_{hh}^2/\mu_R^2; M_{hh}^2/\mu_F^2) + \mathcal{O}(1/N)\,.\end{aligned} \tag{2.8}$$

All the large logarithmic corrections are exponentiated in the Sudakov factor Δ_N, only depending on the dynamics of soft gluon emissions from the initial state partons. It can be expanded as

$$\begin{aligned}\ln \Delta_N\left(\alpha_{\rm S}, \ln N; \frac{M_{hh}^2}{\mu_R^2}, \frac{M_{hh}^2}{\mu_F^2}\right) = {} & \ln N\; g^{(1)}(\beta_0 \alpha_{\rm S} \ln N) + g^{(2)}(\beta_0 \alpha_{\rm S} \ln N, M_{hh}^2/\mu_R^2; M_{hh}^2/\mu_F^2) \\ & + \alpha_{\rm S}\; g^{(3)}(\beta_0 \alpha_{\rm S} \ln N, M_{hh}^2/\mu_R^2; M_{hh}^2/\mu_F^2) \\ & + \sum_{n=4}^{+\infty} \alpha_{\rm S}^{n-2}\; g^{(n)}(\beta_0 \alpha_{\rm S} \ln N, M_{hh}^2/\mu_R^2; M_{hh}^2/\mu_F^2)\,.\end{aligned} \tag{2.9}$$

The term $\ln N\; g^{(1)}$ resums all the LL contributions $\alpha_{\rm S}^n \ln^{n+1} N$, $g^{(2)}$ collects the NLL terms $\alpha_{\rm S}^n \ln^n N$, $\alpha_{\rm S}\, g^{(3)}$ contains the NNLL terms $\alpha_{\rm S}^{n+1} \ln^n N$, and so forth. The perturbative

JHEP08(2018)156

coefficients $g^{(n)}$ needed to perform NNLL resummation are known and only depend on the type of incoming partons, and their explicit expression can be found, for instance, in refs. [25, 26].

All the contributions that are constant in the large-N limit are contained in the function $C_{gg}(\alpha_S)$. They originate in non-logarithmic soft contributions and hard virtual corrections, and can be expanded in powers of the strong coupling:

$$C_{gg}(\alpha_S, M_{hh}^2/\mu_R^2; M_{hh}^2/\mu_F^2) = 1 + \sum_{n=1}^{+\infty} \left(\frac{\alpha_S}{2\pi}\right)^n C_{gg}^{(n)}(M_{hh}^2/\mu_R^2; M_{hh}^2/\mu_F^2) \ . \tag{2.10}$$

In particular, in order to perform N^{i}LL resummation we need up to the $C_{gg}^{(i)}$ coefficient. At the same time, this coefficient can be obtained from the N^{i}LO fixed order computation; even more, given that the soft gluon contributions in $C_{gg}^{(i)}$ are universal, the only process dependence enters via the virtual corrections. The explicit (universal) relation between $C_{gg}^{(i)}$ and the loop corrections has been derived up to $i = 2$ in ref. [27], and later at one order higher in ref. [28], and reads (for $\mu_R = \mu_F = M_{hh}$)

$$C_{gg}^{(1)} = C_A \frac{4\pi^2}{3} + 4C_A\gamma_E^2 + \frac{\hat{\sigma}_{\rm fin}^{(1)}}{\hat{\sigma}_0} \ , \tag{2.11}$$

$$\begin{aligned} C_{gg}^{(2)} = C_A^2 \Bigg(& -\frac{55\zeta_3}{36} - 14\gamma_E\zeta_3 + \frac{607}{81} + \frac{404\gamma_E}{27} + \frac{134\gamma_E^2}{9} + \frac{44\gamma_E^3}{9} + 8\gamma_E^4 \\ & + \frac{67\pi^2}{16} + \frac{14\gamma_E^2\pi^2}{3} + \frac{91\pi^4}{144}\Bigg) + C_A N_f \left(\frac{5\zeta_3}{18} - \frac{82}{81} - \frac{56\gamma_E}{27} - \frac{20\gamma_E^2}{9} - \frac{8\gamma_E^3}{9} - \frac{5\pi^2}{8}\right) \\ & + \beta_0^2 \frac{11\pi^4}{3} + C_A \frac{\hat{\sigma}_{\rm fin}^{(1)}}{\hat{\sigma}_0}\left(\frac{4\pi^2}{3} + 4\gamma_E^2\right) + \frac{\hat{\sigma}_{\rm fin}^{(2)}}{\hat{\sigma}_0} \ , \end{aligned} \tag{2.12}$$

where ζ_n represents the Riemann zeta function, γ_E is the Euler number and $\beta_0 = (11C_A - 2N_f)/12\pi$. The infrared-regulated one and two-loop corrections $\hat{\sigma}_{\rm fin}^{(1)}$ and $\hat{\sigma}_{\rm fin}^{(2)}$ can be obtained from the corresponding matrix elements after applying the corresponding subtraction operator. The explicit formulas can be found in ref. [27]. For the particular case of Higgs boson pair production, their explicit expression valid in the HTL can be found in ref. [21], while for the NLL resummation with full M_t dependence we can obtain numerical results for $\hat{\sigma}_{\rm fin}^{(1)}$, and therefore $C_{gg}^{(1)}$, using the publicly available grid interpolation of the two-loop NLO virtual corrections [16].

Finally, in order to fully profit from the knowledge of the fixed order calculation, we implement the corresponding matching. As usual, we expand the resummed N^{i}LL cross section to $\mathcal{O}(\alpha_s^i)$,[1] add the full N^{i}LO cross section, and subtract the expanded result of the resummed one to avoid a double counting of logarithmic fixed order effects, as

$$\sigma^{\rm N^iLL+N^iLO}(s_H, M_{hh}^2) = \sigma_{\rm res}^{\rm N^iLL}(s_H, M_{hh}^2) - \sigma_{\rm res}^{\rm N^iLL}(s_H, M_{hh}^2)\Big|_{\mathcal{O}(\alpha_s^i)} + \sigma^{\rm N^iLO}(s_H, M_{hh}^2) \, . \tag{2.13}$$

[1] Relative to the LO α_S^2 power, which is always understood.

JHEP08(2018)156

$\sqrt{s}$	NLO ($\mu_0 = M_{hh}/2$)	NLL ($\mu_0 = M_{hh}/2$)	$\frac{\delta\text{NLL}}{\text{NLO}}$ ($\mu_0 = M_{hh}/2$)	$\frac{\delta\text{NLL}}{\text{NLO}}$ ($\mu_0 = M_{hh}$)
7 TeV	$5.773\,^{+16.2\%}_{-15.1\%}$ fb	$6.121\,^{+10.9\%}_{-10.3\%}$ fb	6.0%	21.3%
8 TeV	$8.342\,^{+15.7\%}_{-14.6\%}$ fb	$8.801\,^{+10.9\%}_{-10.2\%}$ fb	5.5%	20.1%
13 TeV	$27.78\,^{+13.8\%}_{-12.8\%}$ fb	$28.92\,^{+10.7\%}_{-10.1\%}$ fb	4.1%	16.7%
14 TeV	$32.88\,^{+13.5\%}_{-12.5\%}$ fb	$34.18\,^{+10.7\%}_{-10.1\%}$ fb	3.9%	16.3%
27 TeV	$127.7\,^{+11.5\%}_{-10.4\%}$ fb	$131.3\,^{+10.4\%}_{-9.9\%}$ fb	2.8%	13.4%
100 TeV	$1147\,^{+10.7\%}_{-9.9\%}$ fb	$1166\,^{+11.0\%}_{-9.6\%}$ fb	1.7%	10.2%

Table 1. Fixed order NLO and resummed NLL+NLO predictions for the Higgs boson pair production total cross section, for different collider energies. The scale uncertainties are indicated as superscript/subscript. We also present the size of the resummed contribution relative to the NLO result, for both $\mu_0 = M_{hh}/2$ and $\mu_0 = M_{hh}$.

3 Numerical results

In this section we present the numerical predictions for the LHC and future hadron colliders. We use the values $M_h = 125\,\text{GeV}$ and $M_t = 173\,\text{GeV}$ for the Higgs boson mass and the top quark pole mass, respectively. We do not consider bottom quark contributions, whose contribution at LO is below 1% [29]. We use the PDF4LHC15 sets [30–35] for the parton densities and strong coupling, evaluated at each corresponding perturbative order. The fixed order cross sections are obtained from the implementation of ref. [1], which is based on the publicly available computational framework MATRIX [36].

In the first place, we present in section 3.1 the NLL+NLO predictions. It is worth to point out that, even if more advanced predictions have been obtained for this process (specifically the so-called NNLO_{FTa} defined in ref. [1]), these results represent the most advanced prediction computed in the full theory, i.e. with full M_t dependence.

Based on the knowledge of the threshold enhanced contributions at NLL with full M_t dependence, and in particular on the $\mathcal{O}(\alpha_S^2)$ of its expansion, we can also provide an improved fixed order (approximated) NNLO prediction. This is presented in section 3.2. Finally, we combine the full NLL calculation with the NNLL contributions computed in the heavy top limit. This is presented in section 3.3.

3.1 NLL+NLO with full M_t dependence

The results for the total cross section are shown in table 1 for different center-of-mass energies. We use as the central scale $\mu_0 = M_{hh}/2$, though we also present results for $\mu_0 = M_{hh}$. Scale uncertainties are obtained via the usual 7-point variation, that is $\mu_{R,F} = \xi_{R,F}\,\mu_0$ with $\xi_{R,F} = (2,2), (2,1), (1,2), (1,1), (1,0.5), (0.5,1), (0.5,0.5)$, i.e. omitting antipodal variations.

We can observe that the size of the threshold effects goes down for larger collider energies, as expected from the fact that more energy is available and therefore soft gluon

JHEP08(2018)156

$\sqrt{s}$	$\frac{\text{NLO}(\mu_0=M_{hh}/2)}{\text{NLO}(\mu_0=M_{hh})}-1$	$\frac{\text{NLL}(\mu_0=M_{hh}/2)}{\text{NLL}(\mu_0=M_{hh})}-1$
7 TeV	17.9%	3.0%
8 TeV	17.1%	2.9%
13 TeV	14.7%	2.3%
14 TeV	14.3%	2.2%
27 TeV	11.7%	1.3%
100 TeV	7.7%	−0.6%

Table 2. Ratio between the $\mu_0 = M_{hh}/2$ and $\mu_0 = M_{hh}$ predictions, at NLO and NLL.

contributions become less dominant. As it was also observed in the heavy M_t limit, we can appreciate that the size of the threshold corrections is much larger for $\mu_0 = M_{hh}$, ranging from 21.3% at 7 TeV to 10.2% at 100 TeV. The corresponding values for $\mu_0 = M_{hh}/2$ are 6.0% and 1.7%, respectively. For LHC energies, the soft gluon resummation effects are of the order of 4% for the central scale $\mu_0 = M_{hh}/2$. We can observe a reduction in the scale uncertainties (except for the 100 TeV predictions, where fixed-order and resummed results are comparable), this reduction being stronger for smaller center-of-mass energies. In fact, the NLL relative scale uncertainties remain practically unchanged when varying the collider energy, being always about ±10%.

In table 2 we present the ratio of the central values for the predictions corresponding to $\mu_0 = M_{hh}/2$ and $\mu_0 = M_{hh}$, both for the fixed-order and resummed results. We can observe that the variation is substantially smaller in the resummed case, pointing towards a clear improvement in the stability of the cross section when taking into account the all-orders soft gluon effects.

More details about this stabilization can be observed in figure 1, where we present the dependence of the total cross section on the renormalization and factorization scales, both for independent and simultaneous variations. We can observe that the resummed contributions generate a strong change in the μ_F dependence at fixed μ_R, which partially compensates the variation of the latter when varying both scales at the same time, leading therefore to a much smaller variation for $\mu_R = \mu_F$, and in general to a smaller scale uncertainty.

We also present NLL predictions (with $\mu_0 = M_{hh}/2$) for the Higgs pair invariant mass M_{hh}, at 7 TeV, 13 TeV (figure 2), 27 TeV and 100 TeV (figure 3). The lower plots show the ratio to the NLO result. We can see that the effect of the resummed contributions becomes larger as the invariant mass of the system increases, which again is expected due to the fact that less energy is available for extra emission. The increase in the Sudakov factor is however partially compensated by a suppression at large M_{hh} in the NLO virtual corrections entering in $C_{gg}^{(1)}$, leading to a rather mild increase in the tail. Also here we can clearly observe that the resummation effects decrease with the collider energy.

It is interesting to compare our results with the ones obtained in the heavy-M_t limit [21]. In order to do so, we present in figure 4 the ratio between the NLL and NLO predictions

JHEP08(2018)156

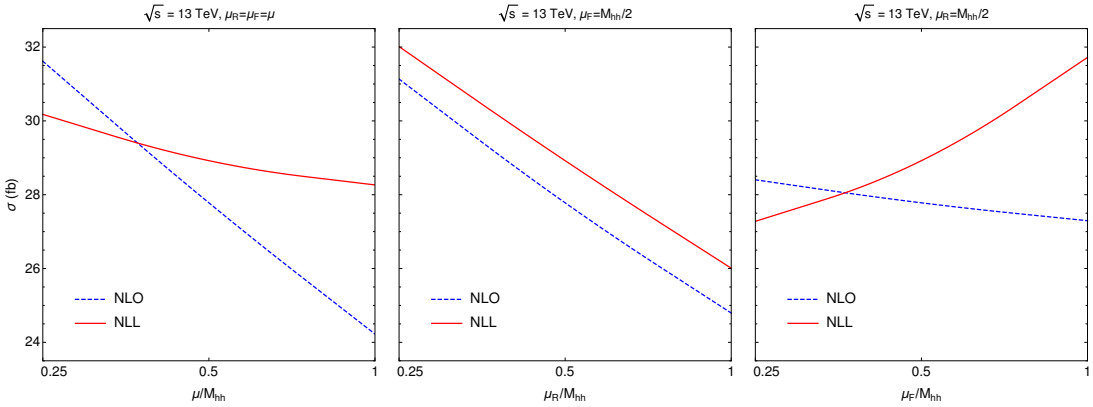

Figure 1. Scale dependence of the total cross section at NLO (blue dashed) and NLL+NLO (red solid), for a collider energy of 13 TeV.

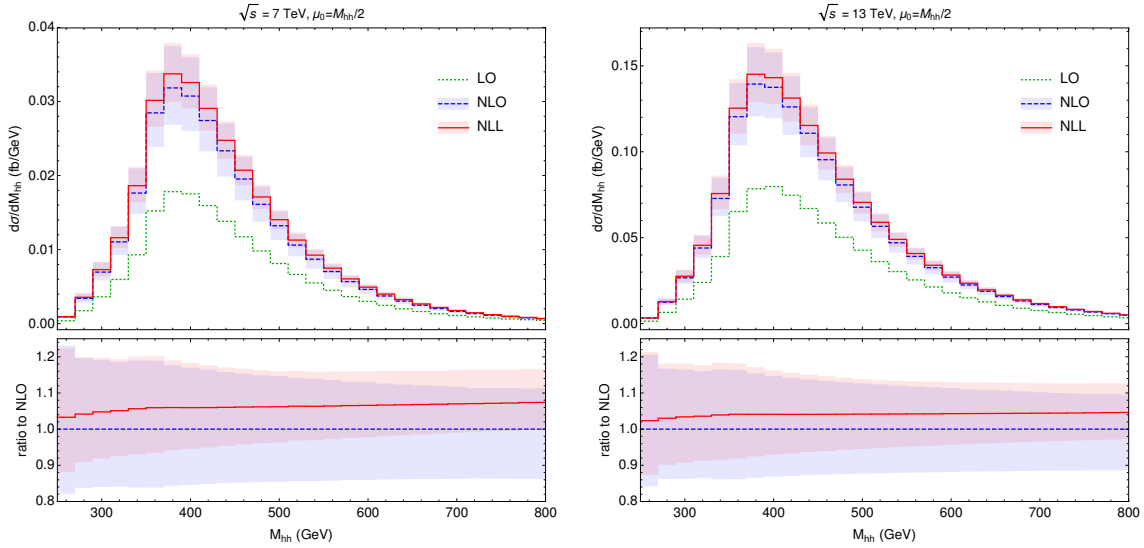

Figure 2. Higgs pair invariant mass distribution at LO (green dotted), NLO (blue dashed) and NLL+NLO (red solid), for collider energies of 7 TeV (left) and 13 TeV (right). The lower panel shows the ratio to the NLO result. The bands indicate the NLO and NLL+NLO scale uncertainties.

as a function of M_{hh} for different collider energies, both in the full theory and in the HTL. We can observe that there are clear differences in the shape, with the results with full M_t dependence growing faster for lower invariant masses but showing a relative suppression with respect to the large-M_t results in the tail. Still, this difference in the M_{hh} spectrum between the two predictions is of the order of $\pm 1\%$, and it is moderate compared to the overall effect of the resummed contributions. This indicates certain stability in the M_t dependence of the threshold effects, and therefore the lack of full M_t dependence at NNLL should lead to a rather small residual uncertainty due to missing finite-M_t effects.

JHEP08(2018)156

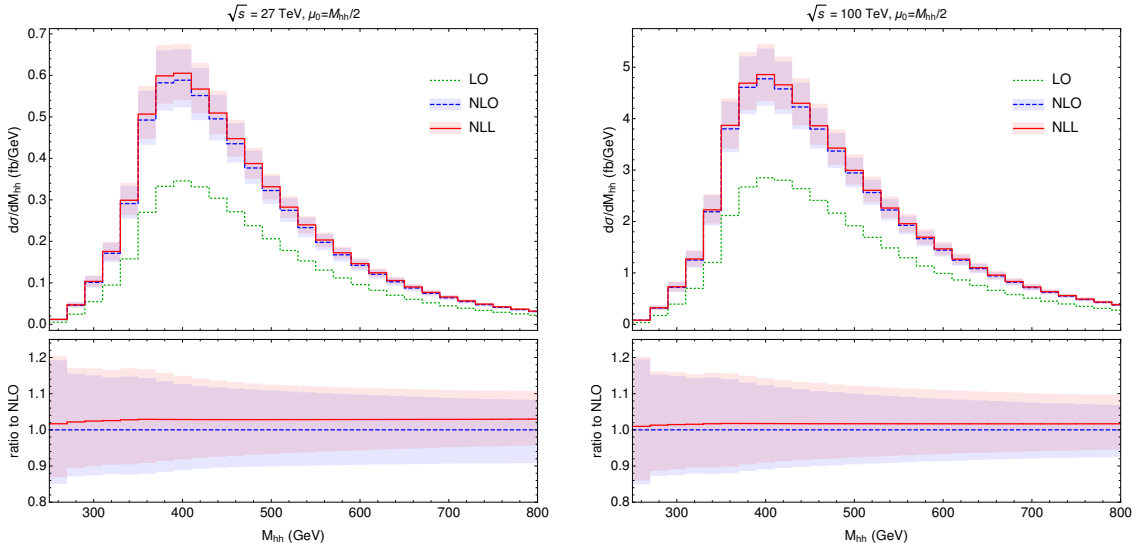

Figure 3. Higgs pair invariant mass distribution at LO (green dotted), NLO (blue dashed) and NLL+NLO (red solid), for collider energies of 27 TeV (left) and 100 TeV (right). The lower panel shows the ratio to the NLO result. The bands indicate the NLO and NLL+NLO scale uncertainties.

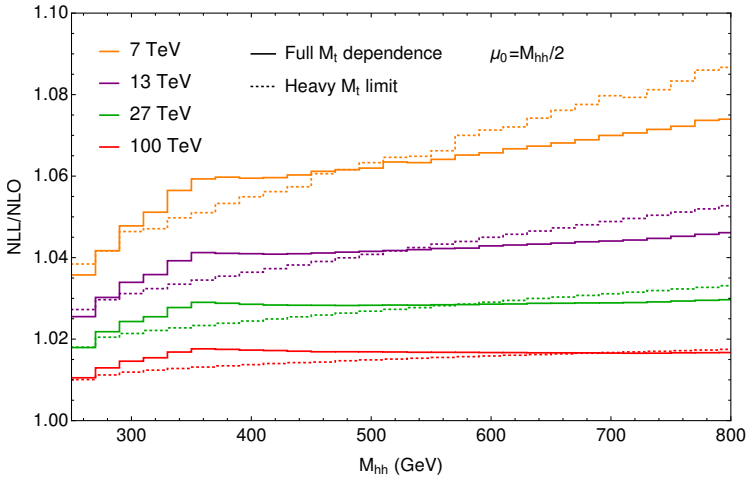

Figure 4. Ratio between the NLL+NLO and NLO predictions, as a function of the Higgs pair invariant mass and for different collider energies. The solid curves show the results with full M_t dependence, while the dashed ones correspond to the large M_t limit.

3.2 Improved NNLO$_{\rm FTa}$

As it was mentioned in the previous section, the NLL+NLO results represent the most advanced prediction available for double Higgs production in the full theory. However, higher order corrections are still sizeable and therefore they need to be included in order to obtain accurate results, even if they are known only in an approximated way. The best fixed order prediction available in the literature is the so-called NNLO$_{\rm FTa}$ [1], which is obtained by working in the heavy M_t limit but improved via a reweighting technique in order to

JHEP08(2018)156

$\sqrt{s}$	7 TeV	8 TeV	13 TeV	14 TeV	27 TeV	100 TeV
NNLO_{FTa} [fb]	$6.572\,^{+3.0\%}_{-6.5\%}$	$9.441\,^{+2.8\%}_{-6.1\%}$	$31.05\,^{+2.2\%}_{-5.0\%}$	$36.69\,^{+2.1\%}_{-4.9\%}$	$139.9\,^{+1.3\%}_{-3.9\%}$	$1224\,^{+0.9\%}_{-3.2\%}$
$\text{NNLO}_{\text{FTa}-\text{i}}$ [fb]	$6.547\,^{+3.4\%}_{-6.9\%}$	$9.406\,^{+3.2\%}_{-6.5\%}$	$30.95\,^{+2.9\%}_{-5.5\%}$	$36.57\,^{+2.7\%}_{-5.3\%}$	$139.5\,^{+2.4\%}_{-4.3\%}$	$1221\,^{+2.0\%}_{-3.2\%}$
$\text{NNLL}_{\text{FTa}-\text{i}}$ [fb]	$6.633\,^{+3.8\%}_{-3.8\%}$	$9.515\,^{+3.7\%}_{-3.7\%}$	$31.18\,^{+3.3\%}_{-3.6\%}$	$36.83\,^{+3.3\%}_{-3.5\%}$	$140.1\,^{+3.0\%}_{-3.3\%}$	$1223\,^{+2.4\%}_{-2.8\%}$
$\frac{\delta\text{NNLL}_{\text{FTa-i}}}{\text{NNLO}_{\text{FTa-i}}}$	1.3%	1.2%	0.8%	0.7%	0.4%	0.1%

Table 3. Total Higgs boson pair production cross sections at hadron colliders at NNLO_{FTa}, $\text{NNLO}_{\text{FTa}-\text{i}}$ and NNLL+$\text{NNLO}_{\text{FTa}-\text{i}}$ (labeled $\text{NNLL}_{\text{FTa}-\text{i}}$ for brevity), for different center of mass energies. All the results correspond to the central scale $\mu_0 = M_{hh}/2$.

account for finite M_t effects. In particular, the NNLO_{FTa} includes the full double-real loop induced squared matrix elements.

Before presenting combined NNLL+NNLO_{FTa} predictions in the following section, it is worth to discuss possible improvements to the approximated NNLO result of ref. [1] based on the knowledge of the full NLL+NLO result. Expanding the NLL+NLO results to $\mathcal{O}(\alpha_S^2)$ –where an overall α_S^2 from the Born cross section is understood–, we can obtain the exact threshold enhanced contributions proportional to $\alpha_S^2 \ln^2 N$.[2] Even if it features the full double-real corrections, these contributions are obtained only within the (Born-improved) heavy M_t limit in the NNLO_{FTa}, because of the approximation performed in the real-virtual piece of the calculation. Therefore, we can define an improved NNLO_{FTa} (denoted as $\text{NNLO}_{\text{FTa}-\text{i}}$) in the following way[3]

$$\sigma^{\text{NNLO}}_{\text{FTa-i}} = \sigma^{\text{NNLO}}_{\text{FTa}} + \left(\sigma^{\text{NLL}} - \sigma^{\text{NLL}}_{\text{HTL}}\right)\Big|_{\text{only } \mathcal{O}(\alpha_S^2)} . \tag{3.1}$$

In table 3 we show the comparison between the NNLO_{FTa} and $\text{NNLO}_{\text{FTa}-\text{i}}$ predictions for the total cross section. We can observe that the difference is very small, being always below 0.5%. Even if this does not represent a proof of the accuracy of the NNLO_{FTa}, the smallness of this effect points in this direction, and the difference is largely included within the estimated M_t uncertainty reported in ref. [1].

In figure 5 we present the Higgs boson pair invariant mass distribution for both NNLO approximations, for a collider energy of 13 TeV. We can observe that the difference between them is again very small in the whole invariant mass range, slowly growing with M_{hh} but always within the scale uncertainties. This behavior is not surprising since the NNLO_{FTa} is expected to be less accurate for large values of M_{hh}, and also because the difference between NNLO_{FTa} and $\text{NNLO}_{\text{FTa}-\text{i}}$ is only in threshold enhanced terms, which become more relevant for larger invariant masses. We can also observe that the scale uncertainties are larger for the $\text{NNLO}_{\text{FTa}-\text{i}}$ in the tail, being the central value corresponding to $\mu_0 =$

[2] Contributions proportional to $\alpha_S^2 \ln^3 N$ and $\alpha_S^2 \ln^4 N$ are already obtained in an exact way at LL, and are also reproduced with full M_t dependence by the NNLO_{FTa}.

[3] Besides having the full M_t dependence in the $\alpha_S^2 \ln^2 N$ term, the $\text{NNLO}_{\text{FTa}-\text{i}}$ differs from the NNLO_{FTa} result also in the term proportional to $\alpha_S^2 \ln N$, though in this case the full M_t dependence is only in those contributions generated by the NLL resummation.

JHEP08(2018)156

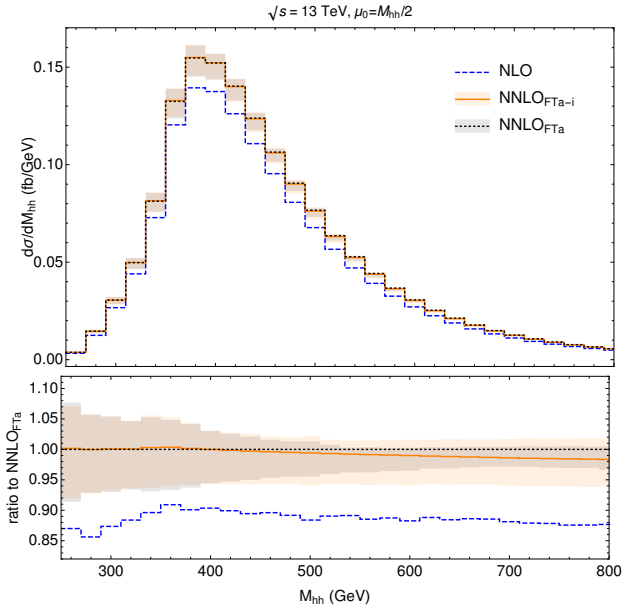

Figure 5. Higgs pair invariant mass distribution at NLO (blue dashed), NNLO_{FTa} (black solid) and $\text{NNLO}_{\text{FTa}-\text{i}}$ (orange dotted), for a collider energy of 13 TeV. The lower panel shows the ratio to the NNLO_{FTa} result. The bands indicate the NNLO_{FTa} and $\text{NNLO}_{\text{FTa}-\text{i}}$ scale uncertainties.

$M_{hh}/2$ in the middle of the uncertainty band, while for the NNLO_{FTa} it is located close to the upper limit. This fact reflects in the slightly larger scale uncertainties for the $\text{NNLO}_{\text{FTa}-\text{i}}$ total cross section that can also be observed in table 3.

In summary, both for the total cross section and the invariant mass distribution we find that the differences between the NNLO_{FTa} and $\text{NNLO}_{\text{FTa}-\text{i}}$ predictions are well within the estimated uncertainties inherent to these approximations.

3.3 NNLL resummation

We present now the NNLL predictions. In order to account for the NLL contributions with full M_t dependence, we add the difference between the full theory and HTL predictions at NLL. Specifically, defining

$$\sigma^{\text{NNLL'}} = \sigma^{\text{NNLL}}_{\text{HTL}} + \sigma^{\text{NLL}} - \sigma^{\text{NLL}}_{\text{HTL}}\,, \tag{3.2}$$

we have that our $\text{NNLL}+\text{NNLO}_{\text{FTa}-\text{i}}$ cross section is given by

$$\sigma^{\text{NNLL+NNLO}}_{\text{FTa-i}} = \sigma^{\text{NNLL'}} - \sigma^{\text{NNLL'}}\Big|_{\mathcal{O}(\alpha_S^2)} + \sigma^{\text{NNLO}}_{\text{FTa-i}}\,. \tag{3.3}$$

For the sake of brevity, we will denote this result $\text{NNLL}_{\text{FTa}-\text{i}}$. Note that the NNLL result is matched to the $\text{NNLO}_{\text{FTa}-\text{i}}$ prediction instead of NNLO_{FTa}, though as it was seen in the previous section the difference between the two is very small.

As an alternative to the approach introduced in eq. (3.2) for the combination of the NLL with full M_t dependence with the NNLL in the HTL, we could define a new NNLL

JHEP08(2018)156

$\sqrt{s}$	$\frac{\text{NNLO}_{\text{FTa-i}}(\mu_0=M_{hh}/2)}{\text{NNLO}_{\text{FTa-i}}(\mu_0=M_{hh})}-1$	$\frac{\text{NNLL}_{\text{FTa-i}}(\mu_0=M_{hh}/2)}{\text{NNLL}_{\text{FTa-i}}(\mu_0=M_{hh})}-1$
7 TeV	7.4%	−1.3%
8 TeV	7.0%	−1.3%
13 TeV	5.9%	−1.3%
14 TeV	5.6%	−1.4%
27 TeV	4.5%	−1.6%
100 TeV	2.8%	−2.1%

Table 4. Ratio between the $\mu_0 = M_{hh}/2$ and $\mu_0 = M_{hh}$ predictions, at $\text{NNLO}_{\text{FTa}-\text{i}}$ and $\text{NNLL}_{\text{FTa}-\text{i}}$.

prediction by directly using the resumation formula evaluating $C_{gg}^{(1)}$ with full M_t dependence and $C_{gg}^{(2)}$ in the large-M_t limit. This different prescription has the same logarithmic accuracy as the one defined by eq. (3.2), and of course agrees with it in the $M_t \to \infty$ limit. We have found that these two approaches agree in the $\mu_0 = M_{hh}/2$ central prediction for the total cross section at the sub-per mille level for all the energies under consideration, being the only noticeable difference the shape of the upper uncertainty band, this one being slightly larger for the prediction defined by eq. (3.2), which therefore we choose in the following in order to be more conservative.

In table 3 we present the $\text{NNLL}_{\text{FTa}-\text{i}}$ predictions for the total cross section, for $\mu_0 = M_{hh}/2$. We can observe that the resummed contributions result in a small increase with respect to the $\text{NNLO}_{\text{FTa}-\text{i}}$ result, ranging from 1.3% at 7 TeV to 0.1% at 100 TeV, and being around 0.8% at the LHC. Again, the effect is much larger for the central scale $\mu_0 = M_{hh}$, where for instance the increase in the total cross section at 13 TeV is above 8%.

From table 3 we can also compare the NNLL predictions with the NNLO_{FTa} results of ref. [1]. We can observe that the increase due to the resummed contributions is partially compensated with the existing decrease from the NNLO_{FTa} to the $\text{NNLO}_{\text{FTa}-\text{i}}$ predictions, accidentally making the difference between the NNLO_{FTa} and $\text{NNLL}_{\text{FTa}-\text{i}}$ results even smaller. The largest difference between these two predictions is in the scale uncertainties, which are comparable in size but turn out to be more symmetric for the $\text{NNLL}_{\text{FTa}-\text{i}}$ result.

In table 4 we compare the fixed order $\text{NNLO}_{\text{FTa}-\text{i}}$ and resummed $\text{NNLL}_{\text{FTa}-\text{i}}$ predictions for the scale choices $\mu_0 = M_{hh}/2$ and $\mu_0 = M_{hh}$. In accordance with what was observed at NLO and NLL, we can see that the fixed order results present a larger variation in the central value when changing the renormalization and factorization scales, while the resummed results show a better stability. Again, this effect is less strong when we increase the collider energy.

Finally, in figures 6 and 7 we present the Higgs pair invariant mass distribution at different collider energies. We can see again that the threshold effects increase with M_{hh} by comparing the $\text{NNLO}_{\text{FTa}-\text{i}}$ and $\text{NNLL}_{\text{FTa}-\text{i}}$ curves. We observe that also at a differential level that the difference between the NNLO_{FTa} and $\text{NNLL}_{\text{FTa}-\text{i}}$ predictions is very small, being below or around 1% in the mass range under study. The difference in the scale uncertainty bands between these two predictions can also be appreciated, specially in the tail.

JHEP08(2018)156

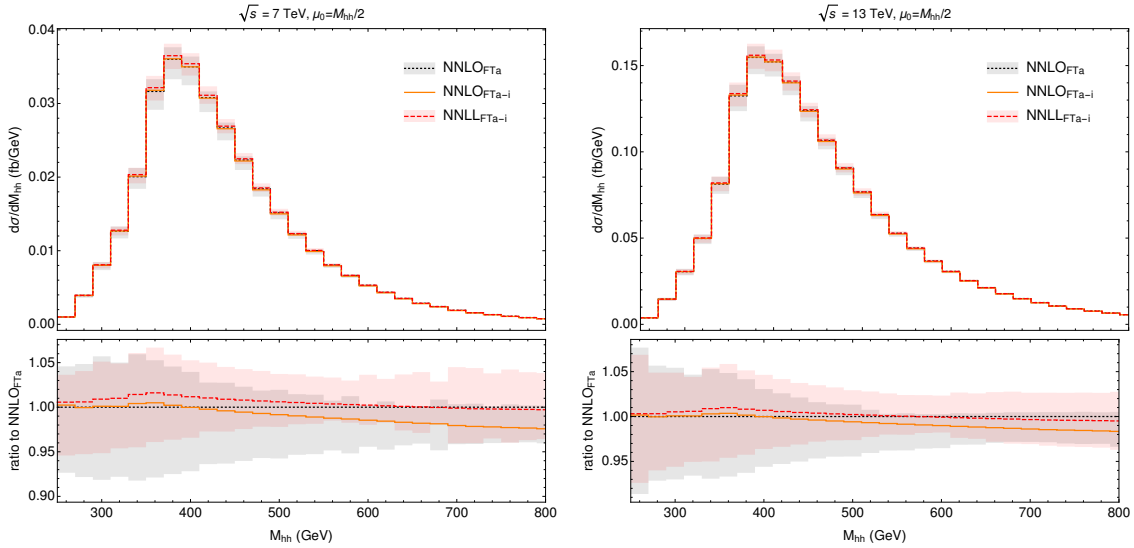

Figure 6. Higgs pair invariant mass distribution at $\mathrm{NNLO}_{\mathrm{FTa}}$ (black dotted), $\mathrm{NNLO}_{\mathrm{FTa-i}}$ (orange solid) and $\mathrm{NNLL}_{\mathrm{FTa-i}}$ (red dashed), for a collider energy of 7 TeV (left) and 13 TeV (right). The lower panel shows the ratio to the $\mathrm{NNLO}_{\mathrm{FTa}}$ result. The bands indicate the $\mathrm{NNLO}_{\mathrm{FTa}}$ and $\mathrm{NNLL}_{\mathrm{FTa-i}}$ scale uncertainties.

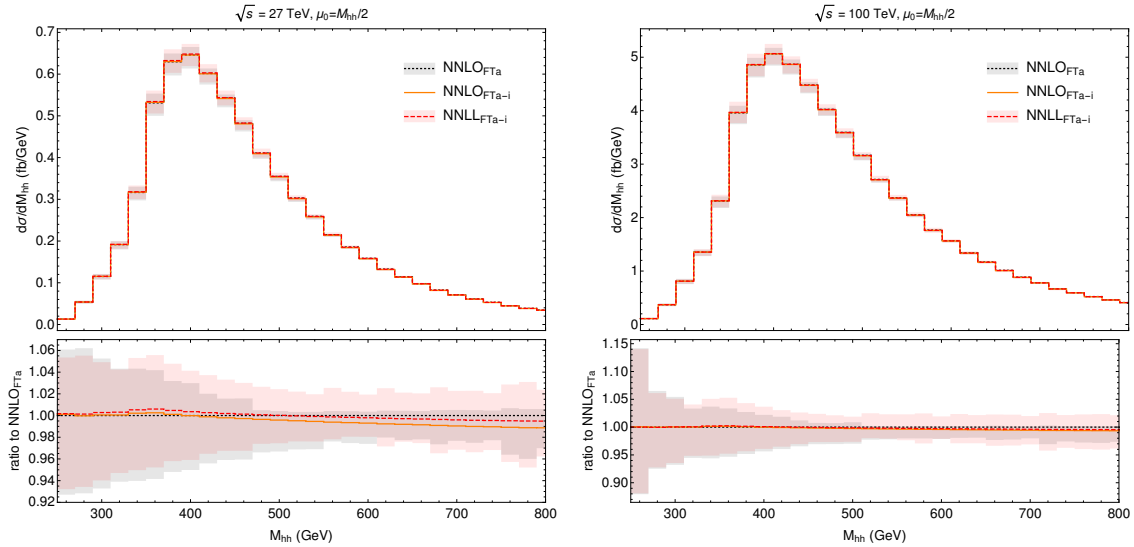

Figure 7. Higgs pair invariant mass distribution at $\mathrm{NNLO}_{\mathrm{FTa}}$ (black dotted), $\mathrm{NNLO}_{\mathrm{FTa-i}}$ (orange solid) and $\mathrm{NNLL}_{\mathrm{FTa-i}}$ (red dashed), for a collider energy of 27 TeV (left) and 100 TeV (right). The lower panel shows the ratio to the $\mathrm{NNLO}_{\mathrm{FTa}}$ result. The bands indicate the $\mathrm{NNLO}_{\mathrm{FTa}}$ and $\mathrm{NNLL}_{\mathrm{FTa-i}}$ scale uncertainties.

In conclusion, the difference between the resummed $\mathrm{NNLL}_{\mathrm{FTa-i}}$ prediction and the $\mathrm{NNLO}_{\mathrm{FTa}}$ result turns out to be small for $\mu_0 = M_{hh}/2$ compared to the size of the theoretical uncertainties, except only for the effect in the shape of the scale uncertainty bands. The small impact of the all orders soft gluon resummation is an indication of the good control over the perturbative expansion.

JHEP08(2018)156

4 Summary

In this work we have computed the threshold resummation for Higgs boson pair production at hadron colliders via gluon fusion, including finite M_t effects. We presented results both at NLL and NNLL accuracy, consistently matched to the corresponding fixed order cross sections.

Our NLL+NLO predictions retain the full M_t dependence, and represent the most advanced prediction for this process computed in the full theory, i.e. not relying on the large-M_t limit. We found that at 13 TeV the NLL+NLO cross section is larger than the NLO result by about 4.1% for the central scale $\mu_0 = M_{hh}/2$, while this effect goes up to 16.7% for $\mu_0 = M_{hh}$. The size of the resummed contributions decreases with the energy, going down to 2.8% and 1.7% at 27 and 100 TeV respectively, again for $\mu_0 = M_{hh}/2$. We observed clear differences in the shape of the corrections as a function of M_{hh} with respect to the large-M_t result, but moderate compared to the overall size of the threshold effects.

Using the knowledge of the full NLL contributions, we have defined an improved NNLO approximation, $\text{NNLO}_{\text{FTa}-\text{i}}$. We found that the difference with respect to the NNLO_{FTa} of ref. [1] is very small, always below 0.5% for all the collider energies under consideration and well within the estimated M_t uncertainties of the approximation, pointing towards the reliability of the NNLO_{FTa} result.

Finally, we have also consistently combined our full NLL predictions with the NNLL resummation computed in the large-M_t limit, and matched it to the $\text{NNLO}_{\text{FTa}-\text{i}}$ result, thus providing a prediction for the Higgs boson pair production cross section with the most advanced ingredients available to date. We found that the effect of the resummed contributions is small at this order, being about 0.8% at the LHC and smaller for larger collider energies. The effect is again larger for $\mu_0 = M_{hh}$, being around 8.1% at 13 TeV. The small size of the threshold resummation effects at NNLL, specially for $\mu_0 = M_{hh}/2$, is an indication of the fact that the perturbative expansion is under good control, and that no sizeable higher order effects are expected beyond the order reached within this calculation.

Acknowledgments

We would like to thank Massimiliano Grazzini for valuable discussions and Gudrun Heinrich for helpful comments on the manuscript. This research was supported in part by the Swiss National Science Foundation (SNF) under contracts CRSII2-141847, 200020-169041, by the Forschungskredit of the University of Zurich, by Conicet and ANPCyT.

References

[1] M. Grazzini et al., *Higgs boson pair production at NNLO with top quark mass effects*, *JHEP* **05** (2018) 059 [arXiv:1803.02463] [INSPIRE].

JHEP08(2018)156

[2] CMS collaboration, *Projected performance of Higgs analyses at the HL-LHC for ECFA 2016*, CMS-PAS-FTR-16-002 (2017).

[3] ATLAS collaboration, *Study of the double Higgs production channel $H(\to b\bar{b})H(\to \gamma\gamma)$ with the ATLAS experiment at the HL-LHC*, ATL-PHYS-PUB-2017-001 (2017).

[4] O.J.P. Eboli, G.C. Marques, S.F. Novaes and A.A. Natale, *Twin Higgs boson production*, *Phys. Lett.* **B 197** (1987) 269 [INSPIRE].

[5] E.W.N. Glover and J.J. van der Bij, *Higgs boson pair production via gluon fusion*, *Nucl. Phys.* **B 309** (1988) 282 [INSPIRE].

[6] T. Plehn, M. Spira and P.M. Zerwas, *Pair production of neutral Higgs particles in gluon-gluon collisions*, *Nucl. Phys.* **B 479** (1996) 46 [*Erratum ibid.* **B 531** (1998) 655] [hep-ph/9603205] [INSPIRE].

[7] S. Dawson, S. Dittmaier and M. Spira, *Neutral Higgs boson pair production at hadron colliders: QCD corrections*, *Phys. Rev.* **D 58** (1998) 115012 [hep-ph/9805244] [INSPIRE].

[8] D. de Florian and J. Mazzitelli, *Two-loop virtual corrections to Higgs pair production*, *Phys. Lett.* **B 724** (2013) 306 [arXiv:1305.5206] [INSPIRE].

[9] D. de Florian and J. Mazzitelli, *Higgs Boson Pair Production at Next-to-Next-to-Leading Order in QCD*, *Phys. Rev. Lett.* **111** (2013) 201801 [arXiv:1309.6594] [INSPIRE].

[10] J. Grigo, K. Melnikov and M. Steinhauser, *Virtual corrections to Higgs boson pair production in the large top quark mass limit*, *Nucl. Phys.* **B 888** (2014) 17 [arXiv:1408.2422] [INSPIRE].

[11] D. de Florian et al., *Differential Higgs Boson Pair Production at Next-to-Next-to-Leading Order in QCD*, *JHEP* **09** (2016) 151 [arXiv:1606.09519] [INSPIRE].

[12] M. Spira, *Effective Multi-Higgs Couplings to Gluons*, *JHEP* **10** (2016) 026 [arXiv:1607.05548] [INSPIRE].

[13] S. Borowka et al., *Higgs Boson Pair Production in Gluon Fusion at Next-to-Leading Order with Full Top-Quark Mass Dependence*, *Phys. Rev. Lett.* **117** (2016) 012001 [arXiv:1604.06447] [INSPIRE].

[14] S. Borowka et al., *Full top quark mass dependence in Higgs boson pair production at NLO*, *JHEP* **10** (2016) 107 [arXiv:1608.04798] [INSPIRE].

[15] G. Ferrera and J. Pires, *Transverse-momentum resummation for Higgs boson pair production at the LHC with top-quark mass effects*, *JHEP* **02** (2017) 139 [arXiv:1609.01691] [INSPIRE].

[16] G. Heinrich, S.P. Jones, M. Kerner, G. Luisoni and E. Vryonidou, *NLO predictions for Higgs boson pair production with full top quark mass dependence matched to parton showers*, *JHEP* **08** (2017) 088 [arXiv:1703.09252] [INSPIRE].

[17] S. Jones and S. Kuttimalai, *Parton Shower and NLO-Matching uncertainties in Higgs Boson Pair Production*, *JHEP* **02** (2018) 176 [arXiv:1711.03319] [INSPIRE].

[18] R. Frederix et al., *Higgs pair production at the LHC with NLO and parton-shower effects*, *Phys. Lett.* **B 732** (2014) 142 [arXiv:1401.7340] [INSPIRE].

[19] F. Maltoni, E. Vryonidou and M. Zaro, *Top-quark mass effects in double and triple Higgs production in gluon-gluon fusion at NLO*, *JHEP* **11** (2014) 079 [arXiv:1408.6542] [INSPIRE].

[20] D.Y. Shao, C.S. Li, H.T. Li and J. Wang, *Threshold resummation effects in Higgs boson pair production at the LHC*, *JHEP* **07** (2013) 169 [arXiv:1301.1245] [INSPIRE].

JHEP08(2018)156

[21] D. de Florian and J. Mazzitelli, *Higgs pair production at next-to-next-to-leading logarithmic accuracy at the LHC*, *JHEP* **09** (2015) 053 [arXiv:1505.07122] [INSPIRE].

[22] G.F. Sterman, *Summation of Large Corrections to Short Distance Hadronic Cross-Sections*, *Nucl. Phys.* **B 281** (1987) 310 [INSPIRE].

[23] S. Catani and L. Trentadue, *Resummation of the QCD Perturbative Series for Hard Processes*, *Nucl. Phys.* **B 327** (1989) 323 [INSPIRE].

[24] S. Catani, M.L. Mangano, P. Nason and L. Trentadue, *The Resummation of soft gluons in hadronic collisions*, *Nucl. Phys.* **B 478** (1996) 273 [hep-ph/9604351] [INSPIRE].

[25] S. Catani, D. de Florian, M. Grazzini and P. Nason, *Soft gluon resummation for Higgs boson production at hadron colliders*, *JHEP* **07** (2003) 028 [hep-ph/0306211] [INSPIRE].

[26] A. Vogt, *Next-to-next-to-leading logarithmic threshold resummation for deep inelastic scattering and the Drell-Yan process*, *Phys. Lett.* **B 497** (2001) 228 [hep-ph/0010146] [INSPIRE].

[27] D. de Florian and J. Mazzitelli, *A next-to-next-to-leading order calculation of soft-virtual cross sections*, *JHEP* **12** (2012) 088 [arXiv:1209.0673] [INSPIRE].

[28] S. Catani, L. Cieri, D. de Florian, G. Ferrera and M. Grazzini, *Threshold resummation at N^3LL accuracy and soft-virtual cross sections at N^3LO*, *Nucl. Phys.* **B 888** (2014) 75 [arXiv:1405.4827] [INSPIRE].

[29] J. Baglio, A. Djouadi, R. Gröber, M.M. Mühlleitner, J. Quevillon and M. Spira, *The measurement of the Higgs self-coupling at the LHC: theoretical status*, *JHEP* **04** (2013) 151 [arXiv:1212.5581] [INSPIRE].

[30] J. Butterworth et al., *PDF4LHC recommendations for LHC Run II*, *J. Phys.* **G 43** (2016) 023001 [arXiv:1510.03865] [INSPIRE].

[31] NNPDF collaboration, R.D. Ball et al., *Parton distributions for the LHC Run II*, *JHEP* **04** (2015) 040 [arXiv:1410.8849] [INSPIRE].

[32] S. Dulat et al., *New parton distribution functions from a global analysis of quantum chromodynamics*, *Phys. Rev.* **D 93** (2016) 033006 [arXiv:1506.07443] [INSPIRE].

[33] L.A. Harland-Lang, A.D. Martin, P. Motylinski and R.S. Thorne, *Parton distributions in the LHC era: MMHT 2014 PDFs*, *Eur. Phys. J.* **C 75** (2015) 204 [arXiv:1412.3989] [INSPIRE].

[34] J. Gao and P. Nadolsky, *A meta-analysis of parton distribution functions*, *JHEP* **07** (2014) 035 [arXiv:1401.0013] [INSPIRE].

[35] S. Carrazza, S. Forte, Z. Kassabov, J.I. Latorre and J. Rojo, *An Unbiased Hessian Representation for Monte Carlo PDFs*, *Eur. Phys. J.* **C 75** (2015) 369 [arXiv:1505.06736] [INSPIRE].

[36] M. Grazzini, S. Kallweit and M. Wiesemann, *Fully differential NNLO computations with MATRIX*, *Eur. Phys. J.* **C 78** (2018) 537 [arXiv:1711.06631] [INSPIRE].

JHEP08(2018)156